Cell, Vol. 88, 393–403, February 7, 1997, Copyright ©1997 by Cell Press

MLP-Deficient Mice Exhibit a Disruption of Cardiac Cytoarchitectural Organization, Dilated Cardiomyopathy, and Heart Failure

Silvia Arber,* John J. Hunter,† John Ross, Jr.,† Minoru Hongo,† Gilles Sansig,§ Jacques Borg,‖ Jean-Claude Perriard,# Kenneth R. Chien,†‡ and Pico Caroni,*

*Friedrich Miescher Institute
CH-4002 Basel
Switzerland
†Department of Medicine
‡Center for Molecular Genetics
University of California, San Diego
La Jolla, California 92093
§Pharma Research
CIBA
CH-4002 Basel
Switzerland
‖Department of Pharmacology
Université Louis Pasteur
67401 Illkirch Cedex
France
#Institute for Cell Biology
Swiss Federal Institute of Technology
CH-8093 Zurich
Switzerland

Summary

MLP is a LIM-only protein of terminally differentiated striated muscle cells, where it accumulates at actin-based structures involved in cytoarchitecture organization. To assess its role in muscle differentiation, we disrupted the *MLP* gene in mice. *MLP* (−/−) mice developed dilated cardiomyopathy with hypertrophy and heart failure after birth. Ultrastructural analysis revealed dramatic disruption of cardiomyocyte cytoarchitecture. At birth, these hearts were not hypertrophic, but already abnormally soft, with cell-autonomous and MLP-sensitive alterations in cytoarchitecture. Thus, MLP promotes proper cardiomyocyte cytoarchitecture, whose perturbation can lead to dilated cardiomyopathy. In vivo analysis revealed that MLP-deficient mice reproduce the morphological and clinical picture of dilated cardiomyopathy and heart failure in humans, providing the first model for this condition in a genetically manipulatable organism.

Introduction

The striated muscle–specific LIM-only protein MLP (muscle LIM protein) is a conserved positive regulator of myogenic differentiation associated with the actin-based cytoskeleton (Arber et al., 1994; Arber and Caroni, 1996). In the myogenic cell line C2C12, its overexpression promotes myogenic differentiation, whereas suppression of MLP expression by an antisense approach markedly impairs this process (Arber et al., 1994). In developing skeletal muscle, expression coincides with the appearance of the differentiated phenotype, and MLP accumulates during muscle fiber formation. MLP is down-regulated in adult skeletal muscle, where it is reinduced by denervation. In contrast, in the heart, MLP is expressed at high levels in atrial and ventricular myocytes during development and in the adult (Arber et al., 1994).

MLP consists of two LIM double zinc fingers linked by a spacer of 50 residues. The LIM motif is a protein binding interface found in a diverse group of proteins that includes LIM kinases and LIM homeodomain proteins (for reviews, see Sanchez-Garcia and Rabbitts, 1994; Dawid et al., 1995). This motif is frequently found in proteins involved in cell differentiation and cell fate determination, suggesting that LIM-based protein interactions may mediate specific regulatory processes in the cell. The mechanism by which MLP promotes myogenic differentiation is not clear, but our recent findings suggest that it may act as a scaffold protein to promote protein assembly along the actin-based cytoskeleton. This hypothesis was based on the demonstration that single LIM motifs engage in specific binding interactions in the cellular environment and that the second LIM motif of MLP can specifically target interacting proteins to the actin-based cytoskeleton (Arber and Caroni, 1996).

Long-term cardiac and skeletal muscle performance is regulated through feedback mechanisms that link mechanical load to the expression of muscle genes, myofibrillar organization, and muscle fiber size (see e.g., Yamazaki et al., 1995). This is particularly important in the vertebrate heart, where, following an initial proliferative phase (Olson and Srivastava, 1996), growth of muscle mass is exclusively due to the hypertrophic enlargement of postmitotic, terminally differentiated cardiomyocytes. In a clinically significant aspect of this process, the adult heart reacts to increased demands for mechanical work via the activation of an adaptive hypertrophic response that is associated with the induction of a defined subset of muscle genes and expansion of the myofibrillar apparatus (see e.g., Chien, 1996). Although compensatory in its nature, this reaction can lead to cardiac dysfunction and heart failure (Keating and Sanguinetti, 1996). Although a large body of work has suggested the existence of signaling pathways in cardiac myocytes that would couple mechanical stress to muscle gene expression and myofibrillogenesis (e.g., Simpson et al., 1993), the molecular mechanisms that link mechanical load to striated muscle growth are poorly understood. Interestingly, like MLP, the LIM-only protein CRP (cysteine-rich protein), which is highly homologous to MLP and is expressed in smooth muscle cells and activated fibroblasts (Wang et al., 1992), also targets to the actin cytoskeleton (Crawford et al., 1994; Arber and Caroni, 1996). In muscle cells and activated fibroblasts, the possibility exists that mechanisms that involve the actin-based cytoskeleton may link mechanical stress to specific patterns of gene expression and cellular organization (for a review, see Grinnell, 1994). Accordingly, one possibility is that MLP may be involved in the linkage

Table 1. Phenotype of MLP-Deficient Mice

Phenotype	Symptoms	Prevalence (+/− × +/−)	(+/− × −/−)	(−/− × −/−)
Early postnatal	Fatigue, enlarged heart, congestive heart failure (P6–P12)	63% (158/249)	44% (32/73)	35% (39/109)
Adult	Dilated cardiomyopathy with hypertrophy, defective neuromuscular transmission	~100%	~100%	~100%

Defective neuromuscular transmission. Motor strength: (+/+), 47.7 ± 4.3 s; (−/−), 27.6 ± 2.6 s (N = 6). Decrement in evoked motor response (high frequency stimulation): (+/+), no reduction during 5 trains; (−/−), 11–14% reduction at 2–3 trains (see also Experimental Procedures).

between tension and muscle growth through the organization of the myofibrillar apparatus and muscle cytoplasm along the actin cytoskeleton.

To define the role of MLP in myogenic differentiation, we have generated MLP-deficient mice. Such mice have soft hearts, with disruption of cardiomyocyte cytoarchitecture at birth. Similar defects were detected in cultured newborn cardiomyocytes, where they could be reversed by forced expression of MLP. After birth, MLP-deficient mice consistently develop dilated cardiomyopathy with hypertrophy and heart failure, and thus provide an animal model for this condition in a genetically modifiable organism. In addition, the results indicate that MLP plays an essential role for proper cardiomyocyte architectural organization and suggest that a pathway to dilated cardiomyopathy may involve intrinsic defects in the cytoarchitecture of cardiomyocytes.

Results

MLP-Deficient Mice Develop Severe Dilated Cardiac Hypertrophy after Birth

During mouse development, MLP is specifically associated with striated muscle, where its expression is detected from the onset of differentiation. As shown in Figure 1A, at E15.5 MLP is specifically expressed in all MyoD-positive skeletal muscles, with the exception of snout muscles. In addition, as mentioned above and in contrast to MyoD, MLP is expressed throughout the developing heart. Expression of MLP in atria and ventricles did not change significantly during development or in the adult. In contrast, *MLP* mRNA levels in mouse skeletal muscle declined markedly during the first two postnatal weeks, and low levels of transcript were detectable in adult skeletal muscle. To examine the role of MLP in muscle formation and growth, we analyzed mice with a targeted disruption of the *MLP* gene. As shown in Figure 1B, the targeting vector contained a neomycin resistance cassette instead of exon 2 that contains the translation initiation site for MLP, and a mutation in an additional internal AUG codon. Three independent recombination-positive embryonic stem cell clones were used to generate MLP-deficient mice, with indistinguishable results. As shown in Figures 1C and 1D, mice homozygous for the disrupted allele expressed no intact *MLP* mRNA and no MLP protein. Mice carrying one copy of the disrupted allele contained markedly reduced levels of MLP (Figure 1D). The immunoblot shown in Figure 1D was probed with an antibody that specifically binds to the carboxyl-terminal end of MLP, thus demonstrating that truncated forms of the protein were also not detectable in *MLP* (−/−) mice.

Expected Mendelian ratios of (+/+), (+/−), and (−/−) animals were present among the offspring of heterozygote brother–sister mating, indicating no significant embryonic lethality (see also Table 1). Mice heterozygous for the disrupted *MLP* allele had no detectable phenotype. In contrast, although *MLP* (−/−) mice displayed no obvious defects at birth, 50–70% of them developed signs of fatigue between postnatal day 5 (P5) and P10 and died within 20–30 hours from the onset of these symptoms. In the following sections, these mice will be referred to as early phenotype mice (Table 1). MLP-deficient mice that did not die during the second postnatal week developed to adulthood and were viable (adult phenotype mice). Second postnatal week mortality was higher in crosses between heterozygous (45–65%) than homozygous (30–40%) animals, suggesting that the penetrance of the early phenotype was affected by the genetic background of *MLP* (−/−) mice. In contrast, as indicated in Table 1, the adult phenotype was nearly 100% penetrant. It included severe defects in cardiac function and structure (see below). In addition, a marked impairment in sustained performance of the limb musculature was detected (Table 1).

Closer examination of *MLP* (−/−) mice revealed selective defects in striated muscle structure and function. Although both skeletal and cardiac muscle lacked rigor, defects were most dramatic in the heart, which showed strikingly decreased tone and became obviously enlarged during postnatal life (Figure 2). At birth, MLP-deficient hearts were already deficient in rigor (see also next sections), but displayed no differences in heart-to-body weight ratios (see Figure 2C for postnatal day 3 data). Subsequently, mice with the early phenotype rapidly developed dramatically enlarged hearts (Figures 2A and 2B), whereas heart size growth was more gradual and less pronounced in the remaining MLP-deficient mice (Figure 2C). As shown in Figure 2B, when compared to body weight, the hearts of early phenotype mice were 2- to 4-fold heavier than control. Significantly, enlargement affected the four heart chambers to a similar extent (Figure 2A, Table 2). This finding and the fact that in wild-type mice MLP is expressed in all cardiomyocytes (in situ hybridization data for adult mouse heart not shown; see Figure 1A for expression at E15.5) suggested that the phenotype was due to an intrinsic cardiac defect.

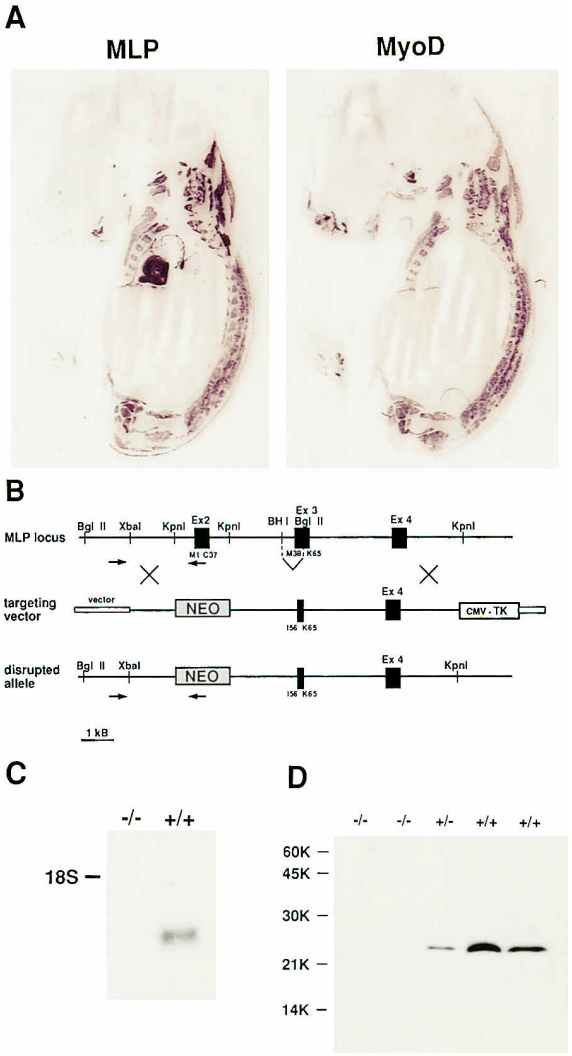

Figure 1. Embryonic Expression of MLP and Generation of a Null Allele at the MLP Locus

(A) In situ localization of mouse MLP and MyoD transcripts on serial sagittal sections of E15.5 mouse embryos. MLP is coexpressed with MyoD in skeletal muscles, with the exception of the snout muscles. Note the strong expression of MLP, but not MyoD, in the developing myocardium (arrow).

(B) Generation of an MLP null allele by homologous recombination. Schematic representation of the *MLP* locus, the targeting vector, and the disrupted allele. Arrows indicate locations of the PCR primers used to verify the presence of the endogenous allele (top) and correct homologous recombination in the *MLP* locus (bottom).

(C) Northern blot analysis of total RNA from the heart of an adult MLP-deficient mouse (−/−) and a control littermate (+/+). The probe contained the first two exons of MLP.

(D) MLP protein is absent in MLP-deficient mice. Western blot analysis of heart homogenates of neonatal MLP-deficient, MLP heterozygous (+/−), and control (+/+) mice. Detection with antibody against a carboxyl-terminal peptide of MLP (Arber et al., 1994).

Two Phases of High Susceptibility for Dilated Cardiac Hypertrophy in MLP-Deficient Mice

To better define the cardiac phenotype of MLP-deficient mice, we carried out a detailed analysis of hypertrophy-associated genes and heart weight in early and late phenotype mice. To determine whether the dramatically enlarged hearts of early phenotype mice displayed gene markers associated with hypertrophic growth, we compared the expression of *ANF* (atrial natriuretic factor) mRNA (a marker of hypertrophy) to that of the ventricular form of myosin light chain-type 2 (MLC-2v, a constitutive myofibrillar protein gene) in control and MLP-deficient mice. As shown in Figure 2B (left panel), *ANF* mRNA was markedly elevated in the ventricles of early phenotype hearts. Strong induction was also detected for muscle ankyrin repeat protein (MARP; designated as clone 4 in Arber et al., 1994) transcript, a novel hypertrophy-associated gene. In contrast, no significant induction of MLC-2v or actin transcripts was detected. Figure 2C shows some characteristics of the cardiac hypertrophic response in late phenotype MLP-deficient mice. For the first two postnatal weeks, the data include all mice with no obvious signs of fatigue (see Experimental Procedures). As shown in the panel on the right, starting around 2 weeks after birth, these mice had hearts consistently larger than controls (130–190%), whereas body weight values were indistinguishable from control (data not shown). As shown in Figure 2C (left panel), the hearts of adult *MLP* (−/−) mice had mRNA patterns characteristic of the cardiac hypertrophy response. In summary, therefore, all MLP-deficient mice develop a marked cardiac hypertrophy reaction, and the two subgroups of mice differ in their susceptibility to a massive and lethal response during the second postnatal week.

MLP-Deficient Cardiac Myocytes Have Major Defects in Cytoarchitectural Organization

Why do MLP-deficient mice develop dilated cardiomyopathy with hypertrophy? The fact that MLP expression is restricted to striated muscle strongly suggested that this was due to a primary defect at the level of the cardiac myocytes. The overall protein composition of the heart on one-dimensional SDS polyacrylamide gels was normal, and no elevated levels of heart muscle enzymes were detected in the serum of adult *MLP* (−/−) mice (data not shown). In sharp contrast to these normal findings, ultrastructural analysis revealed a dramatic disruption of cardiac myofibrillar organization in the absence of MLP (Figure 3). Besides the obvious deficiency in the organized assembly of the myofibrillar apparatus, abnormal features included a pronounced increase in nonmyofibrillar space, ribosomes, sarcoplasmic reticulum, and extracellular space. This disorganization of cardiomyocyte cytoarchitecture was consistently detected throughout the hearts of MLP-deficient mice. Qualitatively similar alterations in ultrastructure have been described for the late phases of dilated cardiomyopathy in humans, albeit usually not to such a dramatic extent. Similarities between the two conditions also extend to characteristic alterations in the distribution of vinculin (Figure 3), a protein involved in the anchorage of the actin-based cytoskeleton to the cell membrane. Thus, like in heart failure with dilated cardiomyopathy, in the cardiomyocytes of *MLP* (−/−) mice, punctate vinculin immunoreactivity consistently extended into the cytosol, and adherens junction immunoreactivity was

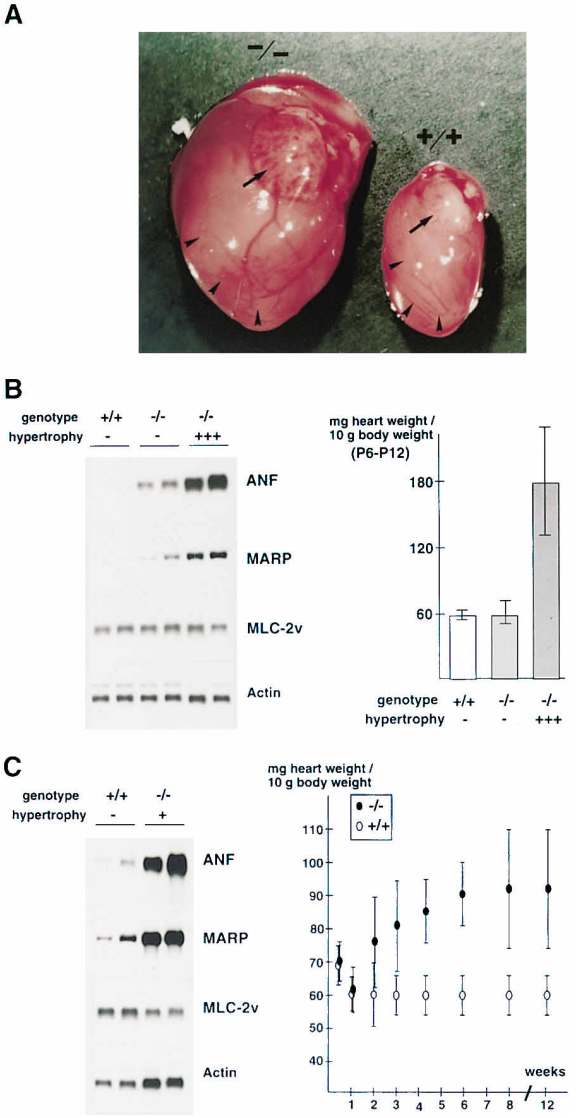

Figure 2. Severe Dilative Enlargement and Hypertrophic Responses of the Heart in MLP-Deficient Mice

(A) Hearts from *MLP* (−/−) and (+/+) littermates were excised from animals at P7, when signs of fatigue were detectable in the MLP-deficient mouse (early phenotype). The heart from the *MLP* (−/−) mouse was four times heavier, whereas body weight was 40% lower than control. Note that both ventricles (arrowheads) and atria (arrows) were greatly enlarged.

(B) Massive hypertrophy reaction in MLP-deficient mice with early phenotype (genotype [−/−]; hypertrophy +++). Left: Northern blot analysis of total RNA from hearts of P10 mice. Probes: ANF, MARP, MLC-2v, and actin (all isoforms). Right: Heart-to-body weight ratios in P6–P12-old animals. Note absence of elevated levels for MLP-deficient mice without signs of fatigue (genotype [−/−]; hypertrophy −). N = 15.

(C) Late phenotype mice develop hypertrophic hearts during the third and fourth postnatal weeks. Left: Northern blot analysis of total RNA from adult (6 week-old) hearts; right: Heart-to-body weight ratios. Mice with signs of fatigue were excluded from this analysis (first two postnatal weeks). $3 \leq N \leq 7$.

stronger and broader. In further analogy to the human disease, the hearts of adult (but not early postnatal) phenotype mice had prominent signs of interstitial cell

Table 2. Enlargement and Dilation of the Left Ventricle in Late Phenotype MLP-Deficient Mice

	EDD (mm)	PWT (mm)	HW/BW	LVW/BW	Lung (g)	Liver (g)
MLP (−/−)						
Mean	4.97[a]	0.51[a]	0.0097[a]	0.0043[b]	0.30[b]	1.71
SD	0.73	0.06	0.0027	0.0004	0.07	0.43
n	9	9	9	4	9	9
MLP (+/−)						
Mean	3.94	0.65	0.0061	0.0036	0.21	1.55
SD	0.39	0.06	0.0012	0.0008	0.02	0.34
n	9	9	10	5	10	10
MLP (+/+)						
Mean	3.90	0.64	0.0056	0.0032	0.22	1.63
SD	0.36	0.06	0.0010	0.0004	0.03	0.34
n	10	10	10	5	10	10

Ten week-old mice were analyzed. Echocardiographic analysis of the left ventricle: EDD, end-diastolic diameter; PWT, left ventricular posterior wall thickness. Weight values: HW/BW, heart-to-body weight ratio; LVW/BW, left ventricular-to-body weight ratio.

[a] $p < 0.004$ versus (+/−) and (+/+).

[b] $p < 0.02$ versus (+/−) and (+/+).

proliferation and fibrosis (Figure 3, Masson's trichrome stain). These results indicate that MLP-deficient mice develop dilated cardiomyopathy with ultrastructural and histological features similar to those found in human patients. Significantly, however, alterations in the organization of the actin cytoskeleton and myofibrillar apparatus were already detectable in the hearts of newborn MLP-deficient mice (Figure 4A), i.e., at a time when the heart tissue was already abnormally soft, but not obviously heavier. These findings suggest that in these mice some disorganization of cardiomyocyte cytoarchitecture precedes an overt hypertrophic response.

To determine whether the cardiac phenotype of *MLP* (−/−) mice was intrinsic to heart muscle cells and cell-autonomous, we analyzed cultures of newborn ventricular myocytes. When compared to controls, cardiomyocytes from *MLP* (−/−) mice consistently spread over a larger area (Figure 4B; 1280 ± 175 μm^2, versus 707 ± 101 μm^2 in controls; 3 day cultures, N = 80) and had unusually high numbers of pseudopodia. As shown in Figure 4C, they displayed alterations in the overall organization of the actin−based cytoskeleton. After 5 days in the presence of the β-adrenergic agonist isoproterenol, MLP-deficient cardiomyocytes had a lacerated appearance, suggestive of impaired resistance to mechanical stress (Figure 4D). Significantly, similar irregular outlines were detected in freshly isolated adult cardiomyocytes from *MLP* (−/−) hearts (Figure 4E), indicating that the overall organization of cardiomyocytes was severely perturbed in the absence of MLP, both in situ and in isolation. These findings indicate that the absence of MLP affected myofibril organization and overall cardiomyocyte cytoarchitecture in a cell-autonomous manner.

MLP Accumulates at Lateral Anchorage Sites of Myofibrils and Promotes the Cytoarchitectural Organization of the Cardiomyocyte

To begin to define the mechanism by which MLP affects cardiomyocyte cytoarchitecture, we determined its subcellular localization in the adult heart and in cultured

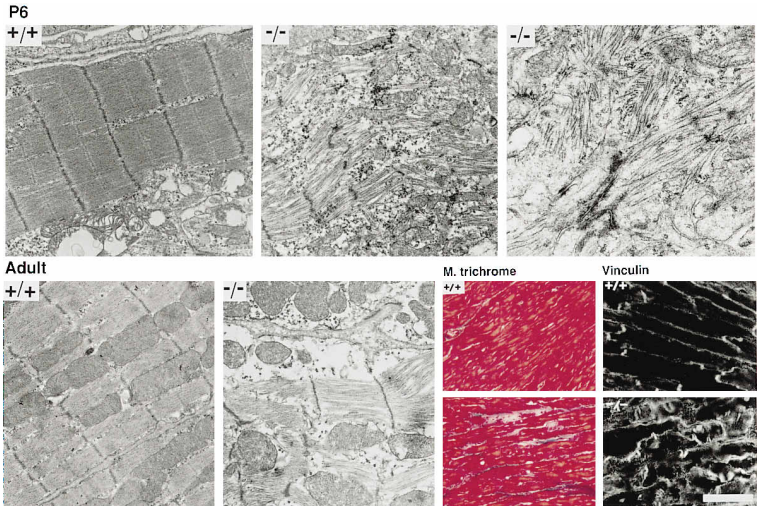

Figure 3. MLP-Deficient Mice Display Dramatic Disruption of Cardiomyocyte Cytoarchitecture, with Myofibrillar Disarray, and Histological Features Resembling Those Found in Patients with Advanced Heart Failure

(Top row) Early phenotype (P6). Electronmicroscopic analysis of sections through a control (+/+) and an MLP-deficient (−/−) heart. (Bottom row) Adult phenotype. Left: Electronmicroscopic analysis of adult hearts; right: Massive fibrosis in adult MLP-deficient hearts (green; Masson's trichrome reaction) and characteristic alterations in the distribution of vinculin immunoreactivity. The bar corresponds to 1.5 μm (P6, left and center), 0.75 μm (p6, right), 1.0 μm (adult, electron micrographs), 90 μm (Masson's trichrome), and 33 μm (vinculin).

cardiomyocytes. As shown in Figure 5A (upper panels), in adult ventricular cardiomyocytes in situ, MLP immunoreactivity was detected in a mainly striate cytosolic pattern, and the signal was highest at vinculin-positive intercellular attachment sites. Because in heart cells vinculin accumulates at adherens junctions, lateral myofibril anchorage sites (i.e., costameres), and Z line–associated structures (e.g., Simpson et al., 1993), the pattern of MLP immunoreactivity suggested that it may be associated with the Z line of myofibrils. This was confirmed by double-labeling immunocytochemistry experiments in cultured cardiomyocytes from newborn *MLP* (+/+) mice, where MLP accumulated in a 2 μm–spaced double-band pattern along myofibrils (Figure 5A, lower panels). Antibodies to sarcomeric α-actinin, the actin-binding protein that links actin filaments from adjacent sarcomeres at the Z line, stained the MLP-negative central section of the double-band, whereas the M band protein myomesin was localized between the MLP double-bands (Figure 5A). Therefore, MLP accumulates in the vicinity of the Z line.

Z line–associated structures are responsible for the lateral alignment of myofibrils and their lateral anchorage at N-cadherin- and vinculin-containing costameres along the cell membrane (e.g., Goncharova et al., 1992). We therefore searched for corresponding perturbations in the absence of MLP. As shown in Figure 5B (upper panels), MLP-deficient cardiomyocytes had elevated contents of irregularly arranged myofibrils. In addition, connexin-43-positive gap junction structures at sites of cell–cell contact were consistently smaller and less well organized (Figure 5B, lower panels). Similar deficits in connexin-43-positive structures at adherens junction sites were detected in freshly isolated cardiomyocytes from adult *MLP* (−/−) mice (data not shown). These findings suggested that MLP may be a crucial component of the anchorage structures involved in the establishment and maintenance of cardiomyocyte cytoarchitecture.

To determine whether MLP promotes proper cardiomyocyte cytoarchitecture, we transfected MLP and related constructs in cultured cardiomyocytes from newborn *MLP* (−/−) mice. As shown in Figure 5C, expression of MLP led to significant organization and simplification of the myofibril pattern in transfected cardiomyocytes. In control experiments, the unrelated protein GAP-43(Ala3,4), a cytosolic and inactive mutant version of the neural growth–associated protein GAP-43 (Widmer and Caroni, 1993), did not promote myofibril organization. MLP consists of the two LIM domains M1 and M2, linked by a 58 amino acid spacer region (Arber et al., 1994). In a previous study, we demonstrated that targeting to the actin cytoskeleton is due to the specific binding properties of the LIM domain M2 of MLP (Arber and Caroni, 1996). Consistent with the actin cytoskeleton properties of the Z line region, the two-LIM construct M2M2 (Arber and Caroni, 1996) bound to Z line structures (Figure 5C), whereas the corresponding M1M1 construct did not (data not shown). Interestingly, in spite of its apparently appropriate subcellular localization, M2M2 did not promote myofibril organization in a manner comparable to that of MLP (Figure 5C). In similar experiments, M1M1 was also inactive (data not shown). Therefore, MLP promotes proper cardiomyocyte cytoarchitecture, and this function requires the binding properties of both LIM domains of MLP. These findings are consistent with our previous hypothesis (Arber and Caroni, 1996) that MLP may function as a scaffold protein to promote the assembly of interacting proteins along the actin-based cytoskeleton.

The Cardiac Phenotype in Adult MLP-Deficient Mice Reproduces the Clinical Features of Cardiomyopathy and Heart Failure in Humans

The combination of cardiac chamber enlargement with myocardial hypertrophy is a typical feature of dilated cardiomyopathy in humans. It was therefore of obvious interest to determine whether MLP-deficient mice reproduce the characteristic features of the condition in humans. To explore this possibility, cardiac morphology and performance in adult MLP-deficient mice was analyzed in vivo utilizing miniaturized physiological technology (Kubalak et al., 1996). Echocardiographic studies showed that in *MLP* (−/−) mice, the left ventricular (LV)

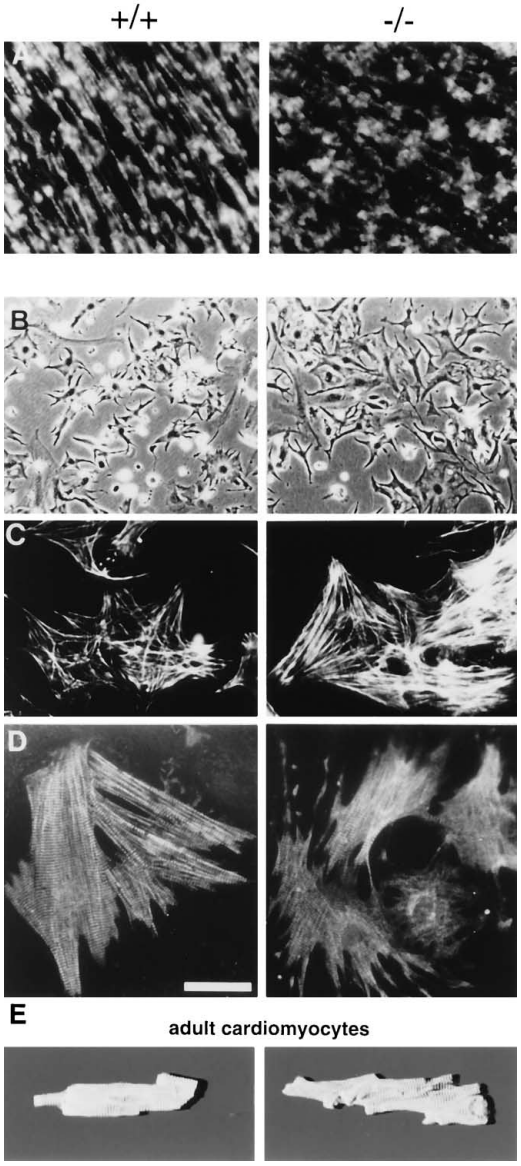

Figure 4. Cytoarchitectural Defects in Newborn MLP-Deficient Hearts, Cultured Newborn Ventricular Cardiomyocytes, and Freshly Isolated Adult Cardiomyocytes

Left: control (+/+); right: MLP-deficient (−/−).

(A) Cryostat sections through neonatal hearts stained for f-actin with rhodamine-phalloidin. Neonatal hearts show signs of myofibrillar disarray.

(B–D) Primary cultures of cardiomyocytes derived from neonatal hearts. (B) shows phase contrast pictures of 3 day cultures. MLP-deficient cardiomyocytes spread over a significantly larger area. (C) shows 1 day cultures stained for f-actin with rhodamine-phalloidin. MLP-deficient cardiomyocytes show higher contents of actin filaments. (D) shows 5 day cultures (myofibrillar C protein stains). Note lacerated appearance of MLP-deficient cardiomyocytes, suggesting impaired resistance to mechanical stress.

(E) 3D confocal reconstructions of myomesin stainings of freshly isolated adult cardiomyocytes. Note lacerated apperance of MLP-deficient cardiomyocytes in situ.

The bar corresponds to 70 μm (A), 150 μm (B), 65 μm (C), 45 μm (D), and 50 μm (E).

chamber was enlarged, the walls thinned, and LV function reduced, indicating impaired function (Figure 6A). The presence of reduced LV performance was evidenced by diminished fractional (%FS) and velocity of LV wall shortening (mean Vcf) (Figure 6B). Despite wall thinning, the ratios of the total heart weight and LV weight to body weight were increased (Table 2), indicating the presence of cardiac hypertrophy, which is an invariable feature in various forms of human heart failure (Kasper et al., 1994). Retrograde catheterization of the LV via the carotid artery in anesthetized, closed-chest mice revealed a marked reduction of the maximum first derivative of LV pressure (LV dP / dt_{max}) in *MLP* (−/−) mice (Figure 6C), clearly demonstrating depression of myocardial contractility. The accompanying reduction in LV dP / dt_{min} (Figure 6C) indicated that LV relaxation was also markedly impaired. Finally, the LV end-diastolic pressure was elevated in *MLP* (−/−) mice (14.1 ± 5 versus 2.2 ± 0.7 mm Hg in control mice, ± SD, $p < 0.02$). These features, together with elevated lung weights (Table 2) suggesting fluid accumulation, are consistent with left ventricular pump failure as seen in human dilated cardiomyopathy (Dec and Fuster, 1994; Kasper et al., 1994). To determine if the *MLP* (−/−) mice displayed the decreased sensitivity of contractility and relaxation to β-adrenergic stimulation observed in human heart failure, the response of LV dP / dt_{max} and LV dP / dt_{min} to graded doses of the β-adrenergic agonist dobutamine was measured. As shown in Figure 6C, the normal response of both contractility and relaxation to β-adrenergic stimulation were abolished in the *MLP* (−/−) mice.

Discussion

Role of MLP in the Organization of the Actin-Based Cytoskeleton of Striated Muscle Cells

A main finding of this study is that disruption of the gene coding for a striated muscle–specific LIM-only protein leads to major alterations in the cytoarchitecture of cardiac muscle cells in vivo and ex vivo. Analysis of neonatal MLP-deficient hearts revealed no obvious abnormalities in overall protein composition, and normal contents of embryonic and neonatal myofibrillar components (e.g., myosin light and heavy chains) and actin isoforms (e.g., α-smooth muscle, cardiac, and skeletal actin) (data not shown). This finding suggested that, rather than directly affecting their transcription or cellular concentration, MLP more likely plays a crucial and specific role in the organization of cytosolic structures in cardiomyocytes. Ultrastructural and light microscopic analysis of skeletal muscle fibers in newborn and adult MLP-deficient mice revealed substantially less pronounced, but qualitatively similar alterations. In addition, MLP-depleted skeletal muscle fibers consistently appeared swollen, and similar defects were detected in cultured myotubes from MLP-deficient mice (data not shown). These alterations were consistent with the reduced rigor of skeletal muscle in these mice and tended to be more pronounced during the first three postnatal weeks and after denervation. It therefore seems that the absence of MLP may affect similar processes in cardiac and

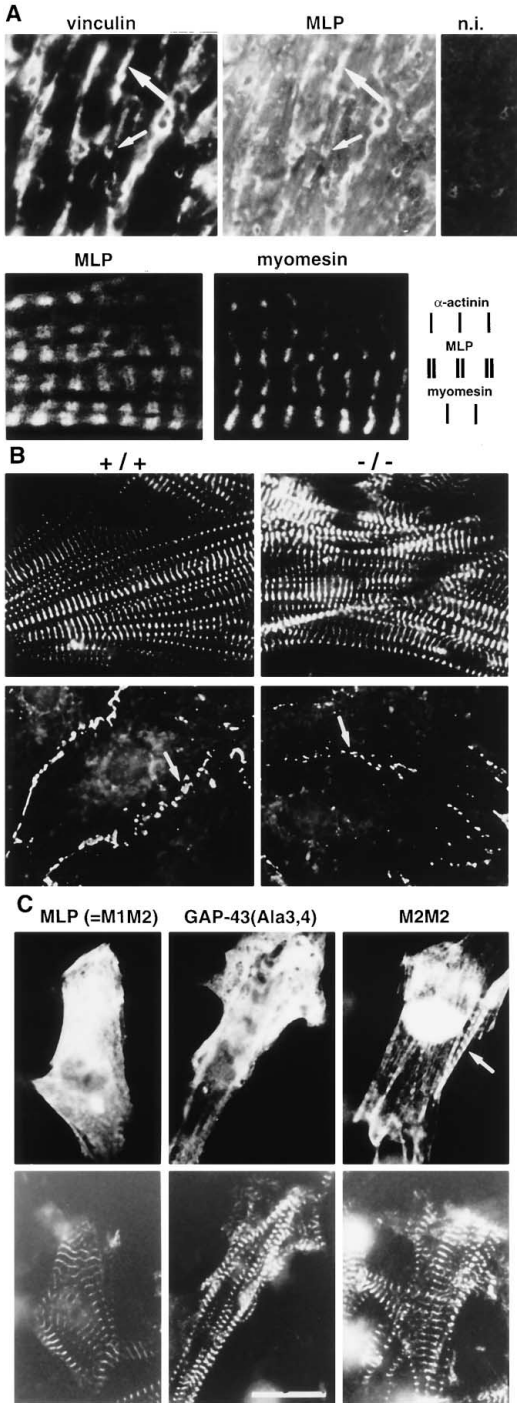

Figure 5. MLP Associates with and Promotes the Organization of Crucial Structures for Cardiomyocyte Cytoarchitecture

(A) MLP codistributes with vinculin-positive anchorage structures at the cell periphery and accumulates at the Z line. Upper panels: Double-labeling immunocytochemistry for vinculin and MLP (cryostat section of adult *MLP* [+/+] heart). Note extensive codistribution with vinculin immunoreactivity (open arrows); the cytosolic labeling pattern for MLP was mainly striated; n.i.: nonimmune serum. Lower panels: Double labeling of cultured newborn *MLP* (+/+) cardiomyocyte for MLP and the M band protein myomesin. MLP associated with myofibrils, where it accumulated in a double-band pattern associated with the Z band region (see schematic representation on the right). In control experiments, cardiomyocytes derived from *MLP* (−/−) mice showed no staining with the MLP antibody (data not shown).

(B) Perturbation of myofibril organization and intercellular junctional structures in cultured MLP-deficient cardiomyocytes. Left: 5 day cultures from newborn *MLP* (+/+) mice; right: 5 day cultures from *MLP* (−/−) mice. Immunocytochemistry for the myofibrillar M band protein myomesin (upper panels) and the gap junction protein connexin-43 (lower panels). Note higher contents of partially disorganized myofibrils and markedly smaller gap junction structures in the absence of MLP (open arrows; the aligned structures are located at sites of contact between cardiomyocytes).

(C) MLP promotes myofibril organization in transfected newborn *MLP* (−/−) cardiomyocytes. After 3 days, transfected cells were double-labeled for transgene (top) and myomesin (bottom). The M2M2 construct (twice the second LIM motif of MLP) bound to Z line structures (open arrow) but, like the control construct GAP-43(Ala3,4), did not attenuate the myofibril phenotype.

The bar corresponds to 58 μm ([A], upper), 5.7 μm ([A], lower), 23 μm ([B], upper), 15 μm ([B], lower), and 20 μm (C).

skeletal muscle cells. Possible reasons for the higher tolerance of skeletal muscle to the absence of MLP include a lower number of membrane attachment sites per sarcomere in this muscle, its much higher degree of cytosolic organization, and the intermittent workload to which it is subjected.

How does MLP affect the organization of myofibrils and related cytosolic structures? One important clue comes from its accumulation at structures (Z lines) that play a crucial role in the establishment and maintenance of cardiomyocyte cytoarchitecture. Thus, myofibrils get organized laterally at the Z line, and their growth, organization, and intercellular alignment involves anchorage sites of the Z line to N-cadherin- and vinculin-positive costameres (e.g., Goncharova et al., 1992). Z line structures are associated with a number of proteins characteristic of f-actin-linked adhesion points and are also responsible for anchorage of the sarcoplasmic reticulum. Our findings that (1) myofibril organization, intercellular gap junction structures, and the overall structural compaction of cardiomyocytes in vivo and in vitro were impaired in the absence of MLP, and that (2) reintroduction of MLP in transfected cardiomyocytes from newborn *MLP* (−/−) mice attenuated the myofibril disorganization phenotype strongly support the notion that MLP is a crucial component of the apparatus involved in the organization and maintenance of cardiomyocyte cytoarchitecture (see model of, Figure 7). When combined to our previous results on the specific binding functions of single LIM motifs (Arber and Caroni, 1996), the transfection results suggest that MLP may function as a scaffold protein to promote the assembly of interacting proteins at Z line structures. Like in transfected nonmyogenic cell lines (Arber and Caroni, 1996), targeting of MLP to actin cytoskeleton–based structures at the Z line appears to require the specific binding properties of the second LIM motif M2. The requirement for the additional function of M1 in the transfection experiments of Figure 5C may reflect binding of MLP to a further crucial component of the anchoring complex.

Interestingly, addition of antibodies against N-cadherin to cardiomyocyte cultures induced myofibrillar and cytosolic disorganization comparable to that detected in MLP-deficient hearts, and these effects were also

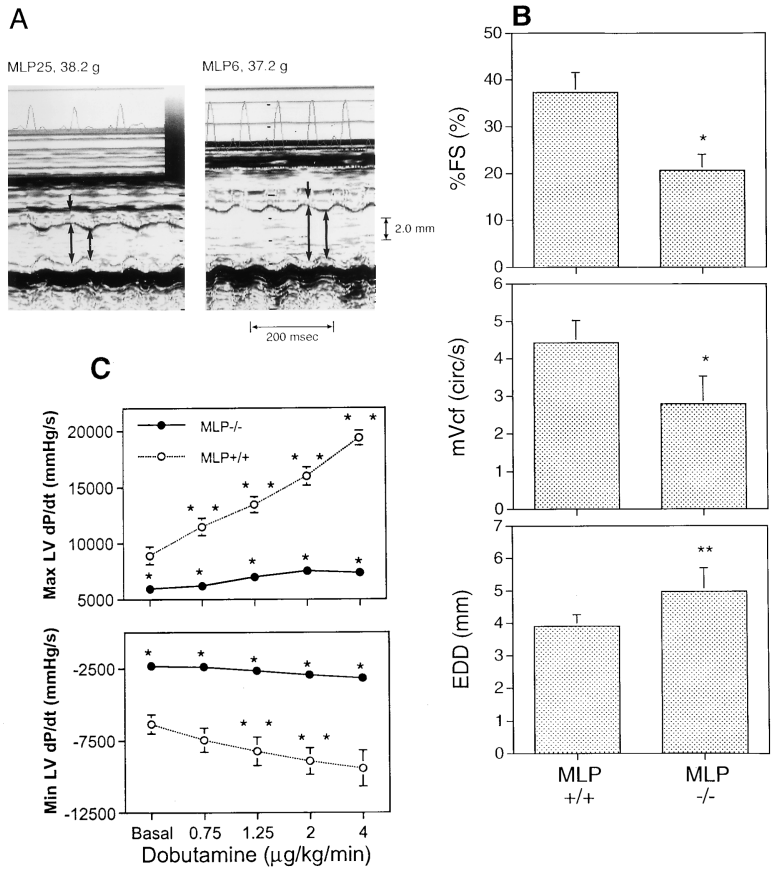

Figure 6. The Cardiac Performance of MLP-Deficient Mice Exhibits Features of Dilated Cardiomyopathy with Heart Failure

(A) Transthoracic M mode echocardiographic tracings in a wild-type (left: MLP25; 38.2 g) and a *MLP* (−/−) mouse (right: MLP6; 37.2 g). Upper tracing in each panel; electrocardiogram. Double-sided vertical arrows indicate internal dimensions of left ventricular (LV) chamber at end-diastole (larger arrow). The smaller adjacent arrow indicates the end of LV ejection. The small vertical arrow indicates anterior edge of intraventricular septal walls. Note thinning of septal and posterior walls, LV dilation, and reduced wall movement in *MLP* (−/−) mouse.

(B) Echocardiographic findings in *MLP* (+/+) and *MLP* (−/−) mice. (%FS) indicates fractional shortening of the LV walls (percentage change in LV diameter from end-diastole to end-ejection). (mVcf) indicates rate of wall shortening. (EDD) indicates end-diastolic diameter. *MLP* (+/+): N = 10; *MLP* (−/−): N = 9. One asterisk indicates $p < 0.001$; two asterisks indicate $p < 0.002$.

(C) Hemodynamic measurements under basal conditions and in response to graded doses of the beta adrenergic agonist dobutamine (DBT; mg/kg/min). Max LV dP / dt: maximum positive first derivative of LV pressure (contractility); Min LV dP / dt: maximum negative first derivative of LV pressure (relaxation). *MLP* (+/+): N = 10 (basal, 0.75, 1.25 DBT), N = 9 (2 DBT), and N = 4 (4 DBT); *MLP* (−/−): N = 7 (basal, 0.75 DBT), N = 6 (1.25, 2 DBT), and N = 3 (4 DBT). Data analyzed with unpaired t test and Bonferroni correction. One asterisk indicates $p < 0.05$ versus MLP (+/+); two asterisks indicate $p < 0.05$ versus basal.

detected for cardiomyocytes that were not in contact with nearby cells (Goncharova et al., 1992; Peralta Soler and Knudsen, 1994). Possibly, signals to the N-cadherin complex from both the outside and the inside (costamere complex, Z line) of the cell regulate cardiomyocyte cytoarchitecture. According to the results of this study, optimal signaling from the inside of the cardiomyocyte would require the presence of MLP. The myogenic cell line C2C12 may be particularly sensitive to this organization process, thus accounting for the fact that it more rapidly formed larger myotubes in the presence of excess MLP and that it was markedly impaired in myotube formation in its absence. Finally, a similar function of MLP may be involved in the organization of the postsynaptic apparatus at the neuromuscular junction, providing a possible rationale for the neuromuscular junction phenotype in MLP-deficient mice.

Susceptibility to Dilated Cardiomyopathy in MLP-Deficient Mice

The most dramatic phenotype in *MLP* (−/−) mice was the appearance of dilated cardiomyopathy with hypertrophy during the first month of postnatal life. Particularly revealing were the extent, the speed, and the chamber-independent characteristics with which this condition developed in mice having the early phenotype. Since we rarely found enlarged hearts in P0–P12 mice without signs of fatigue (Figure 3), all mice with these symptoms died within 20 to 30 hours from their onset, and all of these mice had dramatically enlarged hearts, one must conclude that a 2- to 4-fold increase in heart weight had occurred within 1–2 days. Why only about half of the *MLP* (−/−) mice developed this condition is not clear, but the preliminary analysis of homozygous and heterozygous crosses suggests that genetic background factors may be involved. What drives the dramatic hypertrophic response in the early phenotype *MLP* (−/−) mice? Shortly after birth, the neonatal heart is confronted with an increase in mechanical workload. Specifically, due to the closure of the ductus arteriosus that accompanies the transition from fetal to neonatal life, the left side of the heart is confronted with a sudden and dramatic increase in preload. As a result, a physiological neonatal left ventricular hypertrophic response is activated about 3 days after birth. Remarkably, in MLP-deficient mice the massive hypertrophic response affected all four heart chambers. A possible explanation for these observations is that systemic, chamber wall stress, and local pressure signals may combine to induce and control the hypertrophic response in the heart

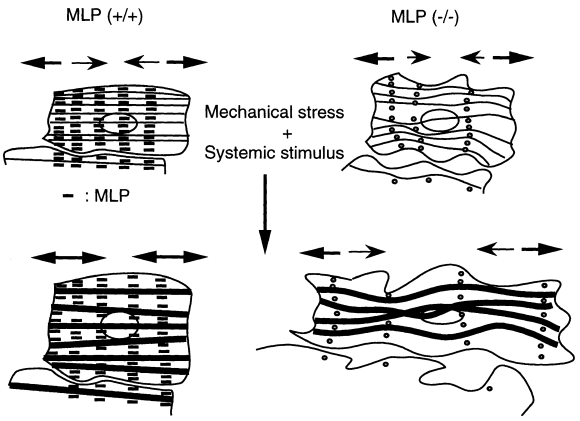

Figure 7. A Model for Development of Dilated Cardiomyopathy with Hypertrophy in the Absence of MLP

MLP is represented by the short bars. Due to the specific binding properties of its second LIM motif, MLP associates with Z line structures involved in the lateral intra- and intercellular alignment of myofibrils, and thus, in the establishment and maintenance of proper cardiomyocyte cytoarchitecture. In the absence of MLP, cardiomyocytes display cytoarchitectural perturbations. Following elevated load demands, systemically acting factors and stress sensors on cardiomyocytes induce and control a compensatory hypertrophic response. In patients with certain mutations in myofibrillar components, diminished sarcomeric performance and the ensuing hypertrophic response lead to hypertrophic cardiomyopathy (Thierfelder et al., 1994), with thickening of chamber walls and reduced chamber volume. In the absence of MLP, deficits in cardiomyocyte cytoarchitectural organization lead to impaired cell and tissue tension. As a result, in the presence of hypertrophic stimuli, cardiomyocytes expand, but still fail to generate sufficient tension to control the hypertrophy response. This leads to a chronic hypertrophic state and to dilated cardiomyopathy.

(see model of, Figure 7). In newborn *MLP* (−/−) mice the heart lacks tonus and presents signs of cytoarchitectural disorganization (Figure 4A). Inability to generate sufficient muscle tension in all MLP-deficient cardiomyocytes and structural deficits in the cellular junctions linking cardiomyocytes lead to cardiac dilation, induction of hypertrophic signals due to excessive stretch, and failure to control the hypertrophic response. MLP may be directly involved in the mechanisms that couple tension to the hypertrophic response. Alternatively, it may play an essential role in the formation and maintenance of the structural substrate required for coupling. This second possibility may be more in keeping with the localization of MLP at structures involved in the lateral intra- and intercellular organization of myofibrils and cardiomyocytes. In both cases, these findings suggest that a cell-autonomous mechanism involving MLP controls the hypertrophic response in cardiomyocytes.

Why do MLP-deficient mice develop dilated cardiomyopathy with hypertrophy? The etiology of this condition in patients is poorly understood, but in some cases there is evidence for a previous viral myocarditis in otherwise healthy patients, with no apparent predisposition for heart disease (Dec and Fuster, 1994; Kasper et al., 1994). The dilated cardiomyopathy that follows these infections appears to develop rapidly and can involve several heart chambers. Although the hearts of newborn MLP-deficient mice were not enlarged, they were already soft, with disorganization of actin-based structures. One possibility, therefore, is that dilated cardiomyopathy develops when the structural integrity of cardiomyocytes and their intercellular contact sites is compromised (Figure 7) (see also Kasper et al., 1994; Keating and Sanguinetti, 1996). In some patients, this may be a consequence of a viral infection, possibly involving autoimmune mechanisms, whereas in MLP-deficient mice, it is due to an intrinsic defect in the absence of MLP.

MLP-Deficient Mice Provide a Model for Dilated Cardiomyopathy and Heart Failure in Humans

The morphological, functional, and molecular features of the cardiac phenotype in *MLP* (−/−) adult mice are undistinguishable from those seen in human heart failure resulting from dilated cardiomyopathy of various etiologies. This clinically important and potentially fatal condition is the convergent phenotype of various diseases that cause loss or dysfunction of cardiomyocytes. Therefore, although yet unidentified hereditary components have been found, it is not typically a genetic disease. The molecular mechanisms leading to the common phenotype of dilated cardiomyopathy are not known and of great interest. The human homologue of *MLP* (*CLP*) has been mapped to 11p15.1 (Fung et al., 1995), a locus that has not yet been associated with human diseases. However, the striking properties of *MLP* (−/−) mice suggest that molecular pathways involving MLP may become dysfunctional during the transition to dilated cardiomyopathy and heart failure. Accordingly, the MLP-deficient model of genetic dilated cardiomyopathy described herein may prove valuable in the identification of pharmacologic agents and other therapies that may retard or reverse the heart failure phenotype (for a review, see Chien, 1996). Its principal value, however, will be for the identification of genes that are involved in the genesis and maintenance of heart failure (e.g., Koch et al., 1995; Zhou et al., 1995; Kubalak et al., 1996) and the application of gene targeting/transgenic techniques to confirm the interactions of other genes with the MLP heart failure phenotype.

Experimental Procedures

Generation of MLP-Deficient Mice

Genomic clones for the generation of a targeting construct were derived from a mouse 129/Sv genomic library (Stratagene), using mouse *MLP* cDNA as a probe. Targeting construct: A 1.2 kb XbaI/KpnI fragment was cloned 5′ to a neomycin cassette driven by the thymidine kinase promoter. A 7 kb KpnI fragment with a 500 bp deletion eliminating M38 of *MLP* was inserted 3′ to the neomycin cassette and 5′ of a CMV promoter–driven thymidine kinase cassette. ES cell clones were screened by PCR using the following primers (see also Figure 1B): sense primer upstream of XbaI site: 5′-GACCCAGGG-CTGTTTGC; antisense primer in deleted genomic region: 5′-ACAATATTGA-CCTGTCCCC; antisense primer in neoresistance cassette: 5′-GTTCAATG-GCCGATCCC. Northern and Western blot analysis of hearts from hetero- and homozygous animals was performed as described previously (Arber et al., 1994). Mice with signs of fatigue (P5–P12, early phenotype; see Figure 3A) were identified due to the striking sluggishness of their movements

and a marked impairment in regaining an upright position when turned on their backs.

Histology and Cell Culture Experiments

For electron microscopy, freshly excised hearts or skeletal muscle were fixed for 1 hr at room temperature in 3% glutaraldehyde, 0.2% tannic acid, in MOPS buffer at pH 6.8 and processed further. Masson's trichrome staining and immunocytochemical labeling of mouse tissues were performed on unfixed cryostat sections, according to standard protocols. Ventricular cardiomyocytes from P0–P1 mice were isolated and cultured according to a modified protocol originally developed for rat heart (Sen et al., 1988). Briefly, minced hearts were digested 3 times with 0.45 mg/ml collagenase (Worthington) and 1.0 mg/ml pancreatin (GIBCO), and dissociated cells were washed and plated on laminin-coated tissue culture plastic in medium consisting of a 3:1 ratio of DMEM / Medium-199 (Sigma), with 10% horse serum and 5% fetal calf serum. One day after plating, serum contents in the medium were reduced to 1% horse serum. Transfections (calcium phosphate method) were carried out 6–8 hr after plating in medium with 4% horse serum. The medium was changed to 1% horse serum 12–16 hr after DNA application, and cells were analyzed 3 days after transfection. Adult cardiomyocytes were isolated, immediately stained, and analyzed as described (Messerli et al., 1993). For immunocytochemistry, cells were prepermeabilized for 10–15 s with saponin, immediately fixed for 20 min at room temperature with 3.7% formaldehyde in PBS, permeabilized for 10 min with 0.1% NP-40, and reacted with antibodies or rhodamine-phalloidin, as described for MLP (Arber et al., 1994). The following cDNA probes were used for Northern blot analysis: ANF, MLC-2v (Chien et al., 1991); MARP, actin, and MyoD (Arber et al., 1994). Antibodies used in this study: rabbit antisera to carboxyl-terminal and internal peptides of MLP (Arber et al., 1994); sarcomeric α-actinin, smooth muscle actin, desmin, vinculin (Sigma); myomesin (monoclonal) and C-protein (antiserum) (Messerli et al., 1993); antiserum to carboxyl-terminal peptide of rat connexin-43 (kind gift from D. Gros, Marseille, France).

Neuromuscular Physiology

The length of time 6- to 8-week-old mice held on to a 32 g grid was recorded; it was reduced by 42% in *MLP* (−/−) mice, with no signs of deterioration when measurements were repeated 1 month later (N = 6). Electromyography measurements in 5–10 week-old mice were performed by stimulating the sciatic nerve at a fixed level along the thigh and recording evoked motor potentials in the gastrocnemius muscle. The maximal amplitude and distal latency of evoked potentials did not differ between wild-type and *MLP* (−/−) mice. To assay for possible defects in neuromuscular transmission, evoked motor potentials were recorded following repetitive stimulation of the sciatic nerve. Five 200 ms stimulations at 3 Hz frequency did not reveal differences between wild-type and *MLP* (−/−) mice. Upon 300 stimulations of 200 ms at 30 Hz, followed by five 3 Hz stimulations at 1 min intervals, *MLP* (−/−) mice displayed clear decrements in the evoked responses to the last five low-frequency stimuli.

Transthoracic Echocardiography, and Hemodynamic Measurements

Mice (1–2 months old) were anesthetized with ketamine (100 mg/kg) and xylazine (2.5 mg/kg) given intraperitoneally, the chest was shaved, and echocardiograms were obtained using an echocardiograph (Apogee CX, Interspec-ATL, Bothell, WA). The transducer (9 MHz) was applied using a gel-filled standoff to obtain two-dimensional guided M-mode tracings of a cross-section of the LV minor axis at the tips of the papillary muscles. These methods and their reliability have been described in detail elsewhere (Tanaka et al., 1996). Within 2 weeks after the echocardiographic study, the mice were anesthetized with ketamine (100 mg/kg) and xylazine (5 mg/kg) (i.p.), the neck was shaved, and a small incision was made in the midline. Under a dissecting microscope, the animals were then intubated and placed on positive-pressure respiration with a 0.5 ml tidal volume at a respiratory rate of 110/min. Both vagal nerves were cut, and catheters were inserted in the left jugular vein for saline infusion and the right carotid artery for measuring aortic pressure with a fluid-filled transducer (Statham P-50). A 1.8 French high fidelity catheter-tip micromanometer (Millar Instruments, Houston, TX) was inserted retrogradely into the aorta via the left carotid artery and advanced until resistance was encountered at the aortic valve. It was then manipulated across the aortic valve into the left ventricle. Following stabilization of hemodynamic conditions, the LV pressure was digitized at a sampling rate of 2000 Hz, and 10 beats were averaged and processed by computer.

Acknowledgments

We are grateful to T. Jessell, W. Krek, and P. Matthias for valuable comments on the manuscript. We thank F. Botteri (Friedrich Miescher Institute, Basel, Switzerland) for substantial help in the generation of the *MLP* (−/−) mice; M. Eppenberger-Eberhardt, E. Perriard, E. Ehler, and M. Schaub (ETH and University Zürich, Switzerland) for help with the cardiomyocyte cultures; M. Azzouz (Université Louis Pasteur, Strasbourg, France) for help with the electromyographic analysis; and U. Saunder (Biocenter, Basel, Switzerland) for help with the electron microscopic analysis. S. A. was supported by a grant from the Swiss Foundation for Research on Muscle Diseases. Parts of this work were supported by a Chair awarded to J. R., Jr. by the San Diego County Affiliate of the American Heart Association and by grants from the National Institute of Health and the National Heart, Lung, and Blood Institute to K. R. C.

Received June 24, 1996; revised December 30, 1996.

References

Arber, S., Halder, G., and Caroni, P. (1994). Muscle LIM protein, a novel essential regulator of myogenesis, promotes myogenic differentiation. Cell *79*, 221–231.

Arber, S., and Caroni, P. (1996). Specificity of single LIM motifs in targeting and LIM/LIM interactions in situ. Genes Dev. *10*, 289–300.

Chien, K.R., Knowlton, K.U., Zhu, H., and Chien, S. (1991). Regulation of cardiac gene expression during myocardial growth and hypertrophy: molecular studies of an adaptive physiologic response. FASEB J. *5*, 3037–3046.

Chien, K.R. (1996). Genes and physiology: molecular physiology in genetically engineered animals. J. Clin. Invest. *97*, 901–909.

Crawford, A.W., Pino, J.D., and Beckerle, M.C. (1994). Biochemical and molecular characterization of the chicken cysteine-rich protein, a developmentally regulated LIM-domain protein that is associated with the actin cytoskeleton. J. Cell Biol. *124*, 117–127.

Dawid, I.B., Toyama, R., and Taira, M. (1995). LIM domain proteins. CR Acad. Sci. (Paris) *318*, 295–306.

Dec, G.W., and Fuster, V. (1994). Idiopathic dilated cardiomyopathy. N. Engl. J. Med. *331*, 1564–1575.

Fung, Y.W., Wang, R.X., Heng, H.H.Q., and Liew, C.C. (1995). Mapping of a human LIM protein (CLP) to human chromosome 11p15.1 by fluorescence in situ hybridization. Genomics *28*, 602–603.

Grinnell, F. (1994). Fibroblasts, myofibroblasts, and wound contraction. J. Cell Biol. *124*, 401–404.

Goncharova, E.J., Kam, Z., and Geiger, B. (1992). The involvement of adherens junction components in myofibrillogenesis in cultured cardiac myocytes. Development *114*, 173–183.

Kasper, E.K., Agema, W.R.P., Hutchins, G.M., Deckers, J.W., Hare, J.M., and Baughman, K.L. (1994). The causes of dilated cardiomyopathy: a clinicopathologic review of 673 consecutive patients. J. Am. Coll. Cardiol. *23*, 586–590.

Keating, M.T., and Sanguinetti, M.C. (1996). Molecular genetic insights into cardiovascular disease. Science *272*, 681–685.

Koch, W.J., Rockman, H.A., Samama, P., Hamilton, R.A., Bond, R.A., Milano, C.A., and Lefkowitz, R.J. (1995). Cardiac function in mice overexpressing the beta-adrenergic receptor kinase or a beta ARK inhibitor. Science *268*, 1350–1353.

Kubalak, S.W., Doevendans, P.A., Rockman, H.A., Hunter, J.J., Tanaka, N., Ross, J., Jr., and Chien, K.R. (1996). Molecular analysis of

cardiac muscle diseases via mouse genetics. In Methods in Molecular Genetics, K.W. Adolph, ed. (San Diego, CA: Academic Press), pp. 470–487.

Messerli, J.M., Eppenberger, M.E., Rutishauser, B., Schwarb, P., Eppenberger, H.M., and Perriard, J.-C. (1993). Remodeling of cardiomyocyte cytoarchitecture visualized by 3D confocal microscopy. Histochemistry *100*, 193–202.

Olson, E.N., and Srivastava, D. (1996). Molecular pathways controlling heart development. Science *272*, 671–676.

Peralta Soler, A., and Knudsen, K.A. (1994). N-cadherin involvement in cardiac myocyte interaction and myofibrillogenesis. Dev. Biol. *162*, 9–17.

Sanchez-Garcia, I., and Rabbitts, T.H. (1994). The LIM domain: a new structural motif found in zinc-finger-like proteins. Trends Genet. *10*, 315–320.

Sen, A.D., Preston, D., Henderson, S.A., Gerard, R.D., and Chien, K.R. (1988). Terminally differentiated neonatal rat myocardial cells proliferate and maintain specific differentiated functions following expression of SV 40 large T antigen. J. Biol. Chem. *263*, 19132–19136.

Simpson, D.G., Decker, M.L., Clark, W.A., and Decker, R.S. (1993). Contractile activity and cell–cell contact regulate myofibrillar organization in cultured cardiac myocytes. J. Cell Biol. *123*, 323–336.

Tanaka, N., Dalton, N., Rockman, H.A., Peterson, K.L., Gottshall, K.R., Hunter, J.J., Chien, K.R., and Ross, J., Jr. (1996). Transthoracic echocardiography in models of cardiac disease in the mouse. Circulation *94*, 1109–1117.

Thierfelder, L., Watkins, H., MacRae, C., Lamas, R., McKenna, W., Vosberg, H.-P., Seidman, J.G., and Seidman, C.E. (1994). α-Tropomyosin and cardiac troponin T mutations cause familial hypertrophic cardiomyopathy: a disease of the sarcomere. Cell *77*, 701–712.

Wang, X., Lee, G., Liebhaber, S.A., and Cooke, N.E. (1992). Human cysteine-rich protein: a member of the LIM/double-finger family displaying coordinate serum induction with c-myc. J. Biol. Chem. *267*, 9176–9184.

Widmer, F., and Caroni, P. (1993). Phosphorylation-site mutagenesis of the growth-associated protein GAP-43 modulates its effects on cell spreading and morphology. J. Cell Biol. *120*, 503–512.

Yamazaki, T., Komuro, I., and Yazaki, Y. (1995). Molecular mechanism of cardiac cellular hypertrophy by mechanical stress. J. Mol. Cell. Cardiol. *27*, 133–140.

Zhou, M.D., Sucov, H.M., Evans, R.M., and Chien, K.R. (1995). Retinoid dependent pathways suppress myocardial cell hypertrophy. Proc. Natl. Acad. Sci. USA *92*, 7391–7395.